Comparative analysis of proximity potentials to describe scattering of ^{13}C projectile off ^{12}C, ^{16}O, ^{28}Si and ^{208}Pb nuclei

M. Aygun
Department of Physics, Bitlis Eren University, Bitlis, Turkey.

Received 4 January 2018; accepted 1 February 2018

In this work, we examine the elastic scattering cross sections of ^{13}C on ^{12}C, ^{16}O, ^{28}Si and ^{208}Pb target nuclei at different incident energies. For the first time, we apply six types of proximity potentials such as Broglia and Winther 1991 (BW 91), Aage Winther (AW 95), Christensen and Winther 1976 (CW 76), Bass 1973 (Bass 73), Bass 1977 (Bass 77) and Bass 1980 (Bass 80) in order to obtain the real part of the optical potential. The imaginary part is taken as the Woods-Saxon potential. Theoretical results are compared with each other as well as the experimental data.

Keywords: Proximity potential; nuclear potential.

PACS: 24.10.Ht; 25.70.-z

1. Introduction

The choice of the nuclear potential is an important parameter to explain the nuclear interactions such as elastic, inelastic and fusion. To produce nuclear potential of any nuclear reaction, different potential forms can be used. With this goal, the phenomenological and double folding potentials [1–4] have been widely applied in theoretical analysis of nuclear interactions. However, investigation of different nuclear potentials is still a hot topic in the field of the nuclear physics. The nucleus-nucleus potential has not yet been unequivocally described [5], although the Coulomb potential due to the charge of the nuclei is well described at the present time. Therefore, the introduction of alternative potentials will be important in explaining different nuclear interactions such as elastic scattering, inelastic scattering, and coupled channels.

In the present study, we are trying to discover alternative potentials to explain scattering cross sections. With this goal, we explore behaviors of proximity potentials in defining the nuclear interaction of two colliding nuclei. These potentials are widely used in fusion calculations [6, 7]. However, as we know from the literature, there is not a comprehensive study about applicability of proximity potentials in determining scattering observables of nuclear reactions. In this context, for the first-time, we employ six different proximity potentials to define the elastic scattering angular distributions of ^{13}C on ^{12}C, ^{16}O, ^{28}Si and ^{208}Pb target nuclei at various incident energies. Then, we compare theoretical results with each other as well as the experimental data.

In next section, a short presentation of nuclear potentials and theoretical calculation is provided. The results and discussion are given in Sec. 3. Section 4 is attributed to the summary and conclusions.

2. Theoretical Formalism

In this section, we give a brief description of optical model (OM) and proximity potentials used in fitting the elastic scattering data of ^{13}C projectile by ^{12}C, ^{16}O, ^{28}Si and ^{208}Pb. We use the OM as the theoretical model. For proximity potentials, we examine six different potentials consisting of Broglia and Winther 1991 (BW 91) [8], Aage Winther (AW 91) [9], Christensen and Winther 1976 (CW 76) [10], Bass 1973 (Bass 73) [11, 12], Bass 1977 (Bass 77) [13] and Bass 1980 (Bass 80) [8].

2.1. Proximity Potentials

2.1.1. Broglia and Winther 1991 (BW 91) potential

In this approach, the real part of the optical potential is assumed as [14]

$$V_N^{BW91}(r) = -\frac{V_0}{\left[1+\exp\left(\frac{r-R_0}{a}\right)\right]} \tag{1}$$

where

$$V_0 = 16\pi\frac{R_1R_2}{R_1+R_2}\gamma a, \quad a = 0.63\,\text{fm} \tag{2}$$

and

$$R_0 = R_1+R_2+0.29, \quad R_i = 1.233A_i^{1/3}-0.98A_i^{-1/3} \tag{3}$$

with surface energy constant γ is

$$\gamma = \gamma_0\left[1-k_s\left(\frac{N_1-Z_1}{A_1}\right)\left(\frac{N_2-Z_2}{A_2}\right)\right], \tag{4}$$

where γ_0 and k_s, respectively are assumed as 0.95 MeV/fm^2 and 1.8.

2.1.2. Aage Winther (AW 95) Potential

The second kind potential employed for the real part is the same as the BW 91 potential except for [14]

$$a = \frac{1}{1.17(1+0.53(A_1^{-1/3}+A_2^{-1/3}))}\text{fm}, \tag{5}$$

and

$$R_0 = R_1+R_2, \quad R_i = 1.2A_i^{1/3}-0.09. \tag{6}$$

2.1.3. Christensen and Winther 1976 (CW 76) Potential

Another form of the real potential analyzed with this work is written as [15]

$$V_N^{CW76}(r) = -50\frac{R_1R_2}{R_1+R_2}\phi(r-R_1-R_2) \quad (7)$$

where

$$R_i = 1.233A_i^{1/3} - 0.978A_i^{-1/3} \quad (i=1,2). \quad (8)$$

The universal function $\phi(s = r - R_1 - R_2)$ is

$$\phi(s) = \exp\left(-\frac{r-R_1-R_2}{0.63}\right). \quad (9)$$

2.1.4. Bass 1973 (Bass 73) Potential

The fourth potential for the real part is parameterized as [15]

$$V_N^{\text{Bass73}}(r) = -\frac{da_sA_1^{1/3}A_2^{1/3}}{R_{12}} \times \exp\left(-\frac{r-R_{12}}{d}\right) \text{MeV}, \quad (10)$$

where

$$R_{12} = 1.07(A_1^{1/3}+A_2^{1/3}),$$
$$d = 1.35 \quad \text{fm} \quad \text{and} \quad a_s = 17 \quad \text{MeV}. \quad (11)$$

2.1.5. Bass 1977 (Bass 77) Potential

Another real potential is in the following form [14]

$$V_N^{\text{Bass77}}(s) = -\frac{R_1R_2}{R_1+R_2}\phi(r-R_1-R_2), \quad (12)$$

where

$$R_i = 1.16A_i^{1/3} - 1.39A_i^{-1/3}. \quad (13)$$

The function $\phi(s = r - R_1 - R_2)$ is assumed as

$$\phi(s) = \left[A\exp\left(\frac{s}{d_1}\right) + B\exp\left(\frac{s}{d_2}\right)\right]^{-1}, \quad (14)$$

where $A = 0.030$ MeV^{-1} fm, $B = 0.0061$ MeV^{-1} fm, $d_1 = 3.30$ fm and $d_2 = 0.65$ fm.

2.1.6. Bass 1980 (Bass 80) Potential

This potential is the same as the Bass 77 potential form. Only the function $\phi(s = r - R_1 - R_2)$ is different and is given by [14]

$$\phi(s) = \left[0.033\exp\left(\frac{s}{3.5}\right) + 0.007\exp\left(\frac{s}{0.65}\right)\right]^{-1}, \quad (15)$$

and

$$R_i = R_s\left(1-\frac{0.98}{R_s^2}\right),$$
$$R_s = 1.28A_i^{1/3} - 0.76 + 0.8A_i^{-1/3} \quad \text{fm} \quad (i=1,2), \quad (16)$$

where $i = 1, 2$ are mass numbers of projectile and target nuclei, respectively.

TABLE I. The W_0 values of the imaginary potential for the BW 91, AW 95, CW 76, Bass 73, Bass 77 and Bass 80 potentials used in the analysis of the ^{13}C + ^{12}C, ^{13}C + ^{16}O, ^{13}C + ^{28}Si and ^{13}C + ^{208}Pb systems.

Reaction	Energy	W_0 (MeV)					
	(MeV)	BW 91	AW 95	CW 76	Bass 73	Bass 77	Bass 80
^{13}C + ^{12}C	250	35	16	33.0	32	10.7	30.0
^{13}C + ^{16}O	50	5.2	13	12.8	3.0	5.20	4.55
^{13}C + ^{28}Si	60	7.3	32	16.5	30	7.70	10.6
^{13}C + ^{208}Pb	390	32	40	42.0	4.0	16.0	52.0

TABLE II. Same as Table I, for r_w values.

Reaction	Energy	r_w (fm)					
	(MeV)	BW 91	AW 95	CW 76	Bass 73	Bass 77	Bass 80
^{13}C + ^{12}C	250	1.25	1.48	1.30	1.10	1.50	1.25
^{13}C + ^{16}O	50	1.39	1.10	1.18	1.40	1.39	1.39
^{13}C + ^{28}Si	60	1.38	1.10	1.38	1.49	1.38	1.38
^{13}C + ^{208}Pb	390	1.28	1.27	1.26	1.10	1.30	1.25

TABLE III. Same as Table I, for a_w values.

Reaction	Energy	a_w (fm)					
	(MeV)	BW 91	AW 95	CW 76	Bass 73	Bass 77	Bass 80
^{13}C + ^{12}C	250	0.3	0.32	0.50	0.70	0.27	0.30
^{13}C + ^{16}O	50	0.5	0.48	0.68	0.60	0.45	0.50
^{13}C + ^{28}Si	60	0.7	0.70	0.80	0.59	0.68	0.68
^{13}C + ^{208}Pb	390	0.5	0.60	0.58	0.70	0.48	0.51

TABLE IV. Same as Table I, for σ values.

Reaction	Energy	σ (mb)					
	(MeV)	BW 91	AW 95	CW 76	Bass 73	Bass 77	Bass 80
^{13}C + ^{12}C	250	1299.7	1631.0	1637.9	1573.3	1542.4	1283.2
^{13}C + ^{16}O	50	1371.3	1263.2	1414.6	1521.0	1297.7	1367.4
^{13}C + ^{28}Si	60	1788.4	1648.8	2237.5	2411.9	1760.7	1877.7
^{13}C + ^{208}Pb	390	3789.3	4046.1	3973.8	2244.3	3594.3	3822.4

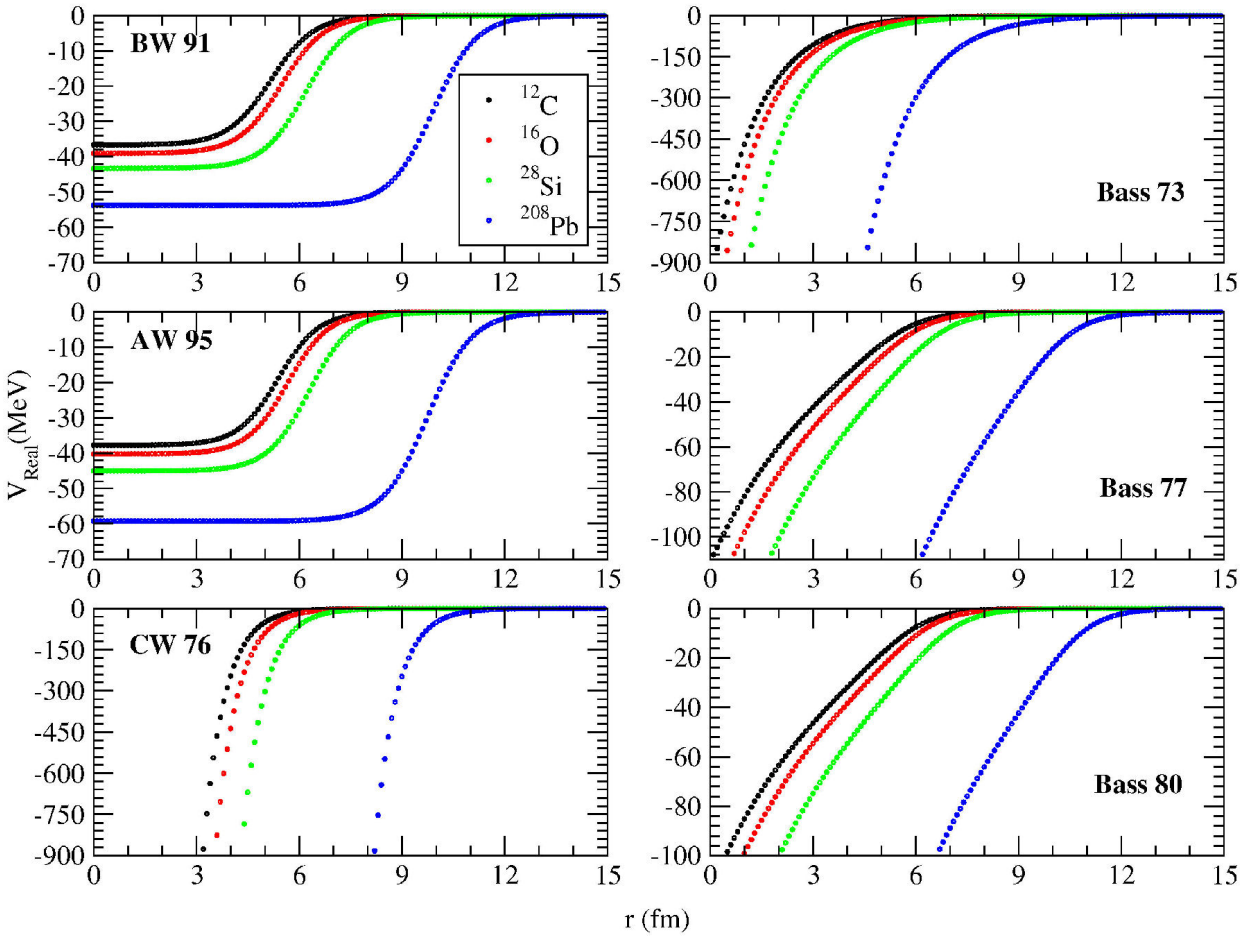

FIGURE 1. Distance-dependent changes of BW 91, AW 95, CW 76, Bass 73, Bass 77 and Bass 80 potentials.

2.2. Optical Model

The OM which has two potentials as the real and imaginary is an efficient model for calculating the elastic scattering cross section. To obtain the real part of the optical potential in our study, proximity potentials have been evaluated. Each of these potentials has been described in the previous section. The imaginary part has been taken as the Woods-Saxon (WS) potential for all the theoretical calculations, which is given by

$$W(r) = \frac{W_0}{\left[1 + \exp\left(\frac{r-R_w}{a_w}\right)\right]}. \quad (17)$$

Thus, the total interaction potential between projectile and target nuclei can be written as

$$V_{\text{total}}(r) = V_{\text{N}}(r) + V_{\text{C}}(r) \quad (18)$$

where V_{N} is nuclear potential and V_{C} is Coulomb potential shown by [16]

$$V_{\text{C}}(r) = \frac{1}{4\pi\epsilon_\circ}\frac{Z_P Z_T e^2}{r}, \quad r \geq R_c \quad (19)$$

$$= \frac{1}{4\pi\epsilon_\circ}\frac{Z_P Z_T e^2}{2R_c}\left(3 - \frac{r^2}{R_c^2}\right), \quad r < R_c \quad (20)$$

where R_c, the Coulomb radius, is $1.25(A_P^{1/3} + A_T^{1/3})$ fm. The code FRESCO has been applied in the OM calculations [17].

3. Results and Discussion

We have examined six versions of proximity potentials to describe the elastic scattering data of ^{13}C + ^{12}C, ^{13}C + ^{16}O, ^{13}C + ^{28}Si and ^{13}C + ^{208}Pb reactions. The distance-dependent variations of the potentials have been shown in Fig. 1. In this context, we have listed the values of W_0, r_w and a_w parameters of the imaginary potential in Tables I, II, and III. In Table IV, we have presented the cross sections (σ) of all the potentials and reactions investigated with this work.

The elastic scattering cross section of ^{13}C + ^{12}C reaction has been analyzed at incident energy of 250 MeV and the theoretical results have been showed in Fig. 2. It has been observed that there is amplitude difference between the results of the potentials with experimental data. It has been noticed that BW 91 and Bass 80 potentials have presented a similar behavior. However, it has been found that the results of CW 76 potential are slightly better than the results of the other potentials.

The angular distribution of ^{13}C + ^{16}O elastic scattering at 50 MeV has been calculated and plotted in Fig. 3. The results are very close together at backwards angles except for the Bass 73 potential. The worst results have been found for

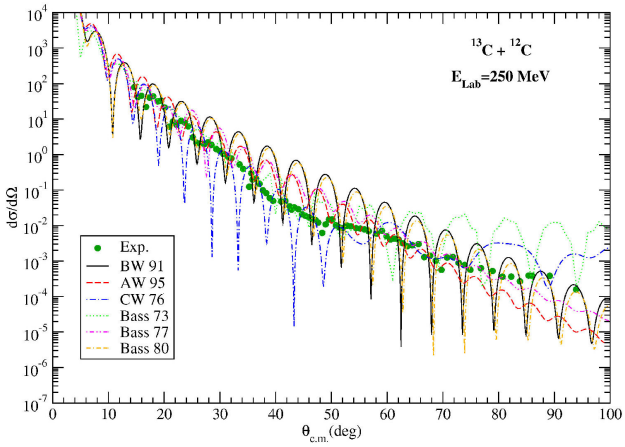

FIGURE 2. Comparison with the experimental data of the ^{13}C + ^{12}C elastic scattering cross sections for the BW 91, AW 95, CW 76, Bass 73, Bass 77 and Bass 80 potentials at $E_{lab} = 250$ MeV. The experimental data have been taken from [18].

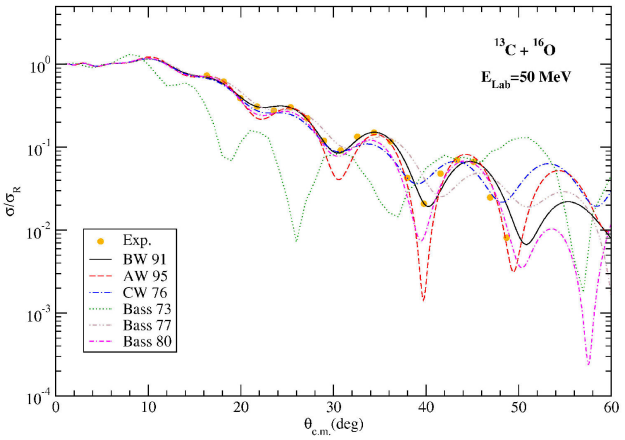

FIGURE 3. The same as Fig. 2, but for the ^{13}C + ^{16}O reaction at $E_{lab} = 50$ MeV. The experimental data have been taken from [19].

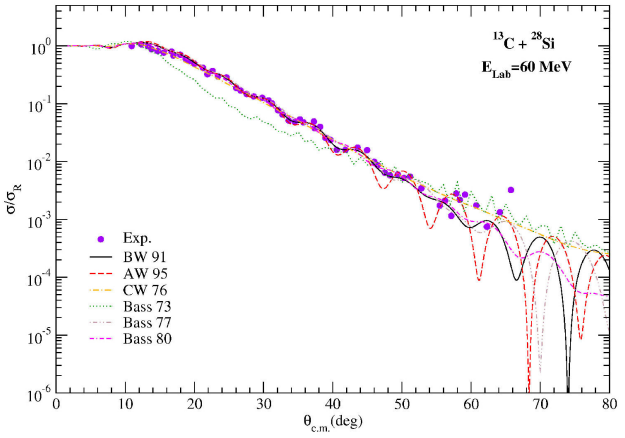

FIGURE 4. The same as Fig. 2, but for the ^{13}C + ^{28}Si reaction at E_{lab}= 60 MeV. The experimental data have been taken from [20].

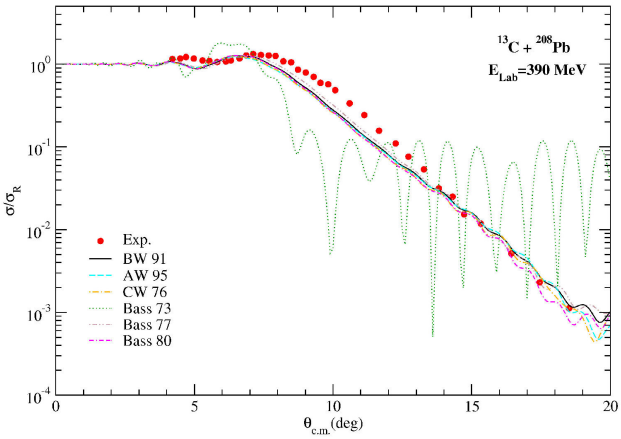

FIGURE 5. The same as Fig. 2, but for the ^{13}C + ^{208}Pb reaction at E_{lab}= 390 MeV. The experimental data have been taken from [21].

the Bass 73 potential. On the other hand, the best results have been obtained with the BW 91 potential.

Another reaction analyzed by using proximity potentials is ^{13}C + ^{28}Si at incident energy of 60 MeV. The elastic scattering results obtained under the OM have been presented in Fig. 4. When the results are compared to each other, the worst results have been found for the Bass 73 potential. However, the BW 91 potential has given slightly better results than the other potentials.

Finally, the elastic scattering data of ^{13}C + ^{208}Pb reaction have been examined via six different nuclear potentials at 390 MeV. The theoretical results have been plotted in Fig. 5. We have observed that the Bass 73 potential have given the worst results compared to the other potentials which are very similar to each other. Moreover, the Bass 77 potential has provided slightly better results than the other potentials.

When we examine the potentials that give the most consistent results with the experimental data for the four different reactions studied, the BW 91 type potential stands out significantly. This potential is basically the potential of the Woods-Saxon type, and the difference is only the method used to determine the potential parameters. It can be said that proximity potential similar to Woods-Saxon type within the scope of BW 91, AW 95, CW 76, Bass 73, Bass 77 and Bass 80 proximity potentials which are generally used to explain fusion reactions is more effective in describing the experimental data.

4. Summary

In this work, we have examined the applicability of proximity potentials to define the elastic scattering cross section. In this respect, we have studied six type proximity potentials to obtain the real part of the optical potential. We have used the WS potential for the imaginary part and have listed all the values of the potential in tables. Then, we have compared the theoretical results with each other as well as the experimental data. We have observed that the results of BW 91 potential are slightly better than the results of the other potentials in general sense. On the other hand, we have noticed that the Bass 73 potential has given the worst results compared to the other potentials. Thus, we have deduced that the theoretical results depend on the choice of the nuclear potentials used in the calculations. We can say that the potentials according to the shapes gives different results with each other and that the harmony with the experimental data increases or decreases.

Consequently, this work provides alternative potential ways to analyze the nuclear interactions. We think that it would be important and useful to investigate more different reactions by using this potentials.

1. M. Aygun, *Rev. Mex. Fis.* **61** (2015) 414-420.
2. M. Aygun, *Rev. Mex. Fis.* **62** (2016) 336-343.
3. M. Aygun, I. Boztosun and K. Rusek, *Mod. Phys. Lett. A* **28** 1350112 (2013).
4. M. Aygun, *Ann. Nucl. Energy* **51** (2013) 1-4.
5. G.R. Satchler, *Nucl. Phys. A* **409** (1983) 3c-20c.
6. G.L. Zhang, W.W. Qu, M.F. Guo, H.Q. Zhang, R. Wolski and J.Q. Qian, *Eur. Phys. J. A* **52** (2016) 39.
7. C.K. Phookan, *Chin. J. Phys.* **55** (2017) 176-186.
8. W. Reisdorf, *J. Phys. G Nucl. Part. Phys.* **20** (1994) 1297.
9. A. Winther, *Nucl. Phys. A* **594** (1995) 203.
10. P.R. Christensen and A. Winther, *Phys. Lett. B* **65** (1976) 19.
11. R. Bass, *Nucl. Phys. A* **231** (1974) 45.
12. R. Bass, *Phys. Lett. B* **47** (1973) 139.
13. R. Bass, *Phys. Rev. Lett.* **39** (1977) 265.
14. G.L. Zhang, Y.J. Yao, M.F. Guo, M. Pan, G.X. Zhang and X.X. Liu, *Nucl. Phys. A* **951** (2016) 86-96.
15. I. Dutt and R.K. Puri, *Phys. Rev. C* **81** (2010) 064609.
16. G.R. Satchler, *Direct Nuclear Reactions* (Oxford University Press, Oxford, 1983).
17. I.J. Thompson, *Comput. Phys. Rep.* **7** (1988) 167.
18. A.S. Demyanova *et al.*, *AIP Conference Proceedings* **1224** (2010) 82-87.
19. N. Ikeda *et al.*, *Eur. Phys. J. A* **7** (2000) 491-502.
20. T. Yamaya *et al. Phys. Rev. C* **37** (1988) 2585.
21. M. Buenerd *et al.*, *Nucl. Phys. A* **424** (1984) 313-334.